Viscoelastic properties of confined polymer films measured *via* thermal wrinkling†

Edwin P. Chan,[a] Kirt A. Page,[a] Se Hyuk Im,[b] Derek L. Patton,‡[a] Rui Huang[b] and Christopher M. Stafford*[a]

Received 6th August 2009, Accepted 23rd September 2009
First published as an Advance Article on the web 8th October 2009
DOI: 10.1039/b916207k

We present a new wrinkling-based measurement technique for quantifying the viscoelastic properties of confined polymer thin films. This approach utilizes real-time laser-light scattering to observe the kinetics of thermally-induced surface wrinkling, which evolves isothermally as a function of annealing time. Specifically, wrinkling is induced by applying a thermal stress to a polystyrene film that is sandwiched between a silicon substrate and an aluminium thin film superstrate. By following the time evolution of the wrinkle wavelength and amplitude, we can infer the rubbery modulus and shear viscosity of the polystyrene film with the aid of a theoretical model.

Polymer thin films are ubiquitous in many technological applications including optics,[1] microelectronics,[2–4] and biomedical devices.[5] In some instances, the performance of these devices depends on the viscoelastic response of the confined polymer films. For example, previous work has shown that the viscoelastic properties at the surface of the polymer dielectric layer can change the morphology of pentacene, thus, altering the transistor performance.[4] Hence, it is essential to understand and control the viscoelastic properties of confined polymer films. Measurement techniques such as nanobubble inflation,[6] dewetting,[7] electrohydrodynamic instability,[8] X-ray photon correlation spectroscopy,[9] and acoustic impedance[10] are capable of measuring the viscoelastic properties of confined polymer films. However, they are limited by (1) the inability to measure both the temperature-dependent modulus and viscosity, and (2) the lack of applicability to small length scales due to their complexity. Thus, it is desirable to develop measurement tools that overcome these limits.

One interesting strategy in measuring the viscoelastic properties of polymer thin films is to take advantage of thermal wrinkling, which is a thermally-induced instability that develops when a polymer film is sandwiched between stiffer, inorganic substrate and superstrate layers. Due to the differences in coefficients of thermal expansion (α) between the polymer and inorganic layers ($\alpha_{polymer} > \alpha_{inorganic}$), a net compressive stress develops at the polymer-superstrate interface when this composite layer is heated to elevated temperatures. At a critical compressive stress, surface wrinkles develop on the superstrate surface characterized by an isotropic morphology that can be approximated as a sinusoidal surface profile.

Based on this approach, previous experimental[11–17] and theoretical[18–21] works have demonstrated that the isothermal time-evolution of the wrinkle wavelength and amplitude is related to the viscoelastic response of the polymer film at the annealing temperature, typically near or above the glass transition temperature of the polymer. In this work, we take advantage of the phenomenon of thermal wrinkling to measure the rubbery modulus and shear viscosity of polystyrene (PS) film as a function of temperature. For this purpose, we use surface laser-light scattering (SLS) to characterize the wrinkled surface in real-time in order to monitor the changes in morphology as a function of annealing time at fixed annealing temperatures. The results from such experiments are compared to a theoretical model, from which the viscoelastic properties of the PS thin film are extracted.

PS thin films were prepared by spin-casting a 600,000 g/mol PS (Polymer Source, Inc§) solution in toluene onto a silicon substrate. The films were then annealed under vacuum for 24 h at 180 °C to remove residual solvent and mitigate the residual stress from processing history. The film thickness was determined to be 270 nm ± 3 nm *via* interferometry (Filmetrics F20 UV, Filmetrics, Inc§). An aluminium (Al) film was then thermally evaporated onto the PS film to form the final composite film. The Al film thickness was determined to be 54 nm ± 1 nm measured *via* atomic force microscopy step height measurements. The composite films were used for thermal wrinkling without additionally processing.

A schematic of the thermal wrinkling process is illustrated in Fig. 1a. The Al/PS composite thin film is heated to elevated

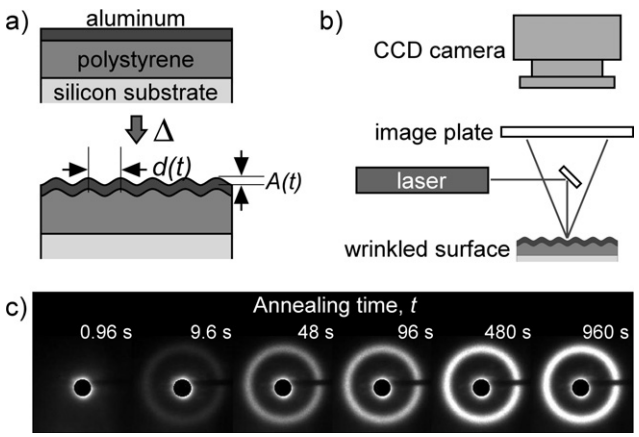

Fig. 1 (a) Schematic of thermal wrinkling approach to measuring the rubbery modulus and viscosity of a confined PS thin film. (b) Schematic of the SLS experimental setup. (c) Representative time-evolved scattering patterning as captured by the SLS at 125 °C.

[a]*Polymers Division, National Institute of Standards and Technology, 100 Bureau Drive, Gaithersburg, MD 20899, USA. E-mail: chris.stafford@nist.gov; Fax: +1 301 975 4924; Tel: +1 301 975 4368*
[b]*Department of Aerospace Engineering and Engineering Mechanics, University of Texas, Austin, TX 78712, USA. E-mail: ruihuang@mail.utexas.edu; Fax: +1 512 471 5500; Tel: +1 512 471 7558*

† Reported data error bars and value uncertainties represent one standard deviation as the estimated standard uncertainty of the measurements.

‡ Present address: School of Polymers and High Performance Materials, University of Southern Mississippi, Hattiesburg, MS 39406, USA.

temperatures until (1) a significant compressive stress develops in the composite film due to the thermal expansion mismatch of the layers, and (2) the polymer gains sufficient mobility that results from heating above its glass transition temperature. At this critical temperature, wrinkles develop on the aluminium film surface characterized by random surface relief patterns with a dominant wavelength and amplitude.[14,17,22,23]

SLS was performed using a custom-built instrument (Fig. 1b). The composite film was placed on a hot stage (Linkam TMS94, Linkam Scientific Instruments), and held at a predetermined annealing temperature ranging from 120 °C to 135 °C in 5 °C increments. This temperature range is above the glass transition temperature of PS ($T_g \approx 105$ °C), which promotes mobility of the PS layer and facilitates wrinkle formation. The 2-dimensional (2-d) scattering images were collected using a charge-coupled device (CCD) camera (Apogee kx260e, Apogee Instruments, Inc) with a time resolution of 0.56 seconds to 0.96 seconds, depending on the annealing temperature. Each 2-d image was radially averaged to determine the scattering intensity as a function of the scattering vector, k. The peak intensity was fitted as a Gaussian and the corresponding scattering vector was determined.

Representative time-resolved scattering images for PS annealed at 125 °C are presented in Fig. 1c. During early annealing times, the scattering profiles are featureless with relatively low intensity. Because wrinkle formation is a kinetic process that depends on the thermal properties of the composite film, we attribute this observation to the initially featureless surface with the wrinkle amplitude below the critical value for SLS. As time progresses, the wrinkle amplitude grows significantly, characterized by an isotropic morphology of a dominant wavelength, d, and amplitude, A. This dominant wavelength is captured by SLS as the scattering vector, $k = (4\pi/\lambda)\sin\theta \approx 2\pi/d$. To a first-order approximation, the wrinkle amplitude is related to the peak intensity, I, and the wavelength of incident light, λ, as $A \approx I^{1/2}(\lambda/2\pi)$.[24]

Experimentally, we observe that both the wrinkle amplitude and wavelength increase with annealing time, t. Fig. 2a summarizes the changes in A and d *versus* t for PS annealed at 125 °C. At a given temperature, A increases with time until a plateau is reached. During early times, A grows exponentially with time at a growth rate, S. From linear perturbation analysis, S is related to the wavelength, d, the materials properties of the Al thin film (h_f, ν_f, E_f), and the PS layer (h_i, ν_i, E_i, η_i).[18,19] Specific to an elastic/viscoelastic composite system that is laterally confined ($h_i/h_f < 10$), the relationship between A, d and S is predicted to be:

$$\frac{dA(t)}{dt} = SA(t) = \left[\frac{\frac{1-2\nu_i}{1-\nu_i}\left(\frac{h_i}{h_f}\right)\left(\frac{E_f}{12(1-\nu_f^2)}\left(\frac{2\pi}{d}h_f\right)^4 - \sigma\left(\frac{2\pi}{d}h_f\right)^2\right) - \frac{E_i}{1+\nu_i}}{2\eta_i}\right]A(t) \quad (1)$$

At long times, the wrinkle growth process reaches a plateau when A becomes commensurate with the Al film thickness due to the nonlinear effects of post-buckling deformation. Thus, the growth rate decreases and eventually reaches an equilibrium state when both A and d approaches a plateau ($A = A_r$, $d = d_r$), which minimizes the elastic energy stored in PS and Al. Physically, this

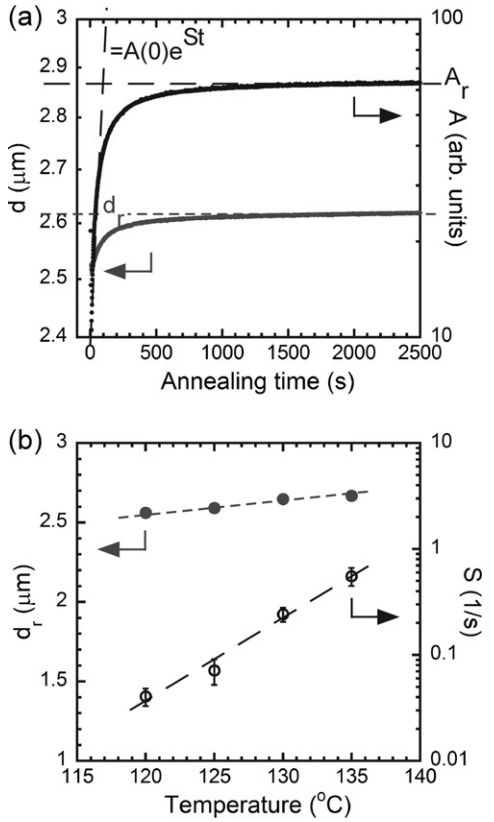

Fig. 2 (a) Representative time-evolved wrinkle wavelength, d, and amplitude, A, for the PS thin film at 125 °C. (b) The key parameters of long time wavelength, d_r, and growth rate, S, extrapolated from (a) that are used to determine the rubbery modulus, $E_{i,r}$, and shear viscosity, η_i.

plateau reflects the long time limit, rubber-like state of the PS film that is characterized by a physically-entangled network of mobile PS chains above its glass transition. The elastic modulus at the rubbery limit, $E_{i,r}$, is determined by applying the equilibrium condition of wrinkling:[21]

$$E_{i,r} = \frac{(1-2\nu_i)(1+\nu_i)}{12(1-\nu_i)}\left(\frac{h_i}{h_f}\right)\left(\frac{2\pi h_f}{d_r}\right)^4 \frac{E_f}{1-\nu_f^2} \quad (2)$$

Hence, eq. (2) implies that $E_{i,r}$ can be measured based on the long time limit of the wrinkle wavelength, d_r.

The key experimentally-measured parameters from the SLS measurements that reflect the viscoelastic properties of the PS film are d_r and S. At long annealing times, measurement of d_r allows for the interpolation of $E_{i,r}$. At short annealing times, measurement of S allows for the interpolation of η_i. Specifically, S is determined at the early stages of the annealing process when an initial value of k is observed. Both parameters increase with annealing temperature (Fig. 2b), and their trends can be explained in the context of several thermally-related processes. Increasing the annealing temperature leads to an enhanced softening of the PS layer. This softening can be attributed to a decrease in the life-time and density of the physical chain entanglements, which act as physical crosslinks. Thus, this softening reduces $E_{i,r}$ as reflected by an increase in d_r, but also reduces the critical stress for wrinkling, σ_c. Additionally, increasing the annealing temperature leads to a reduction in the

shear viscosity and an increase in the thermally-induced compressive stress in the Al film, σ. Therefore, the reductions in η_i and σ_c, coupled with the increase in σ contribute to the observed increase in S with temperature.

By substituting the experimentally measured d_r values and the defined materials properties into eq. (2), we can determine $E_{i,r}$ of PS at a given temperature. The materials constants are: $h_f = 54$ nm, $\nu_f = 0.33$, $E_f = 7 \times 10^{10}$ N/m^2 for the Al thin film, and $h_i = 270$ nm, $\nu_i = 0.495$ for the PS layer. We choose $\nu_i = 0.495$ for PS by assuming that it is a physically-entangled polymer network with sufficient mobility that behaves rubber-like above its T_g.[25,26] Unlike a chemically-crosslinked elastomer whose entanglements are permanent crosslinks, the entanglements for PS are a dynamic network of physical associations, or constraints that restrict polymer motions. Above T_g, the entanglement life-time and density are expected to decrease with increasing temperature, which would lead to a subsequent decrease in the rubbery modulus and shear viscosity. Thus, we expect that this reduction in entanglement density would also change ν_i with annealing temperature. Due to the difficulty in measuring the change in ν_i with temperature, and the convolution of Poisson's ratio and elastic modulus, we choose a constant Poisson's ratio for all the interpolations in this study.

The shear viscosity, η_i, can be determined by substituting S, d, and materials properties into the growth rate relationship from eq. (1).

$$\eta_i = -\frac{\frac{1-2\nu_i}{1-\nu_i}\left(\frac{h_i}{h_f}\right)\left(\frac{E_f}{12(1-\nu_f^2)}\left(\frac{2\pi}{d}h_f\right)^4 + \sigma\left(\frac{2\pi}{d}h_f\right)^2\right) + \frac{E_i}{1+\nu_i}}{2S} \tag{3}$$

The parameter E_i is determined based on the intial value of k that was used in extrapolating S by using eq. (2). However, because k does not evolve noticeably with annealing time, the difference between E_i and $E_{i,r}$ is not significant.

To determine η_i from eq. (3), the compressive stress in the Al film is estimated to be $\sigma \approx -3 \times 10^8$ N/m^2, which is slightly below the yield stress of bulk aluminium.[27] We note that this stress may come from two origins. One is the residual stress within the layers during film processing, and other is the thermal expansion-mismatch induced stresses during the thermal wrinkling experiment. An independent measurement of the compressive stress may be used to improve the accuracy of the estimated value.

Using eq. (2) and (3), we determined the $E_{i,r}$ and η_i values of the confined PS film as function of annealing temperatures, respectively (Fig. 3). Both material properties decrease with annealing temperature, which is consistent with the discussions above. To better illustrate the accuracy of our technique, we compared our results with traditional parallel-plate rheometry. Specifically, we measured the rubbery modulus and shear viscosity of bulk PS using rheometry and the results are compared with the values obtained from thermal wrinkling measurements (Fig. 3). Because the viscoelastic properties of PS are also strain-rate dependent, we compared the results from the two measurement techniques using similar strain rates. We estimated the average strain rate, $\Delta\varepsilon/\Delta t$, in the thermal wrinkling experiments as the ratio of the change in wrinkle amplitude as a function of time *versus* the amplitude, which is coincidently equivalent to the growth rate, S, from eq. (1):

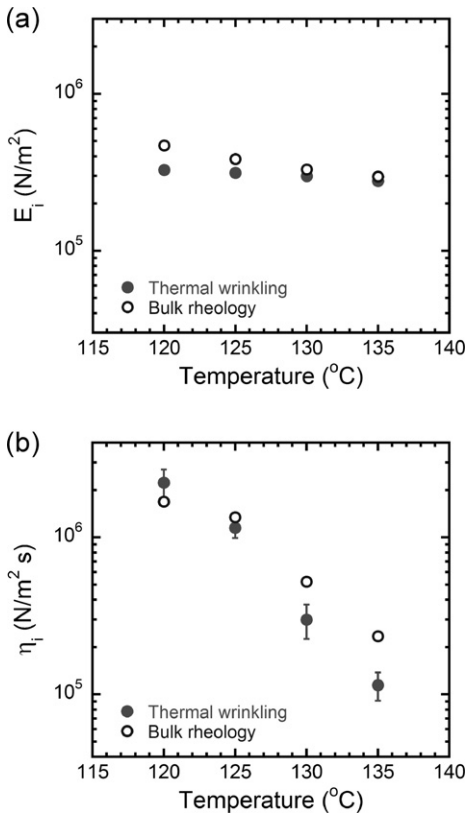

Fig. 3 (a) Summary of rubbery modulus, $E_{i,r}$, as a function of temperature and comparison with bulk rheology. (b) Summary of shear viscosity, η_i, as a function of temperature and comparison with bulk rheology.

$$\frac{\Delta\varepsilon}{\Delta t} \approx \frac{dA(t)/A(t)}{dt} = S \tag{4}$$

The average strain rate, as approximated by S from Fig. 2b, increases with annealing temperature. Comparing the values of $E_{i,r}$ and η_i at similar strain rates, the results from thermal wrinkling are in good agreement with the values from bulk rheometry (Fig. 3). The $E_{i,r}$ values from thermal wrinkling are comparable to the values from bulk rheology. There are slight deviations at the two lower annealing temperatures which we attribute to the discrepancy in the strain rates for the techniques. Because $E_{i,r}$ from thermal wrinkling is measured at relatively long times, the estimated strain rates at these times are lower than the lowest rates used in bulk rheometry (≈ 0.00001 s^{-1} *versus* 0.1 s^{-1}). The η_i values deviate slightly than the bulk values at all annealing temperatures. We attribute the deviations of η_i from bulk to two probable causes. In addition to the previously described discrepency in strain rates between the two techniques, an additional cause for deviation is related to the exact value of the Poisson's ratio for PS during the thermal wrinkling experiments at short times. It is valid to assume ν_i is that of an ideal rubbery network at long annealing times for temperatures above T_g. However, ν_i at short annealing times may be slightly less than an ideal rubbery network due to the viscoelastic response of PS. Therefore, slight changes in ν_i can lead to significant changes in η_i based on the relationship shown in eq. (3).

Conclusions

Thermal wrinkling, combined with SLS, provides a new approach for measuring the viscoelastic properties of confined PS thin films above its glass transition temperature. We showed that by employing the equations established for theoretical buckling mechanics, it is possible to quantify the rubbery modulus and the shear viscosity of a PS thin film under confinement. This technique will provide a new measurement platform in quantifying the temperature-dependent viscoelastic relaxation behavior of a variety of confined polymer systems.

Although we have demonstrated this measurement technique for confined PS films, it is not limited to polymers with a glass transiton. In general, as long as sufficent wrinkling strain is applied, this technique is capable of quantifying the viscoelastic properties of a variety of the polymer systems. Thus, it can be extended beyond polymer systems with a glass transition to materials with phase transitions, such as melting or order–disorder transitions.

Finally, another interesting measurement application of thermal wrinkling is adapting it to probe the effects of confinement on the viscoelastic properties of the polymer thin film. For ultrathin polymer films, thermal wrinkling provides a new approach to measuring local viscoelastic properties of these materials under both substrate and superstrate confinement. We will explore this thin film confinement effect on the viscoelastic properties of amorphous polymers in a future publication.

Acknowledgements

The authors thank Sheng Lin-Gibson for the bulk rheology measurements and Jun Young Chung for insightful discussions. E.P.C. and K.A.P. acknowledge the NIST/National Research Council Postdoctoral Fellowship Program for funding. R.H. and S.H.I. are grateful for financial support by the National Science Foundation under grant no. 0547409. This work is an official contribution of the National Institute of Standards and Technology. The U.S. Government is authorized to reproduce and distribute reprints for Government purposes notwithstanding any copyright notation hereon.

Notes and references

§ The equipment and instruments or materials are identified in the paper in order to adequately specify the experimental details. Such identification does not imply recommendation by NIST, nor does it imply the materials are necessarily the best available for the purpose.

1 U. Schulz and N. Kaiser, *Prog. Surf. Sci.*, 2006, **81**, 387–401.
2 G. Leising, B. Stadlober, U. Haas, A. Haase, C. Palfinger, H. Gold and G. Jakopic, *Microelectron. Eng.*, 2006, **83**, 831–838.
3 M. L. Chabinyc, *J. Vac. Sci. Technol., B*, 2008, **26**, 445–457.
4 C. Kim, A. Facchetti and T. J. Marks, *Science*, 2007, **318**, 76–80.
5 S. Krishnan, C. J. Weinman and C. K. Ober, *J. Mater. Chem.*, 2008, **18**, 3405–3413.
6 P. A. O'Connell and G. B. McKenna, *Science*, 2005, **307**, 1760–1766.
7 G. Reiter, *Macromolecules*, 1994, **27**, 3046–3052.
8 D. R. Barbero and U. Steiner, *Phys. Rev. Lett.*, 2009, **102**, 248303.
9 L. Lurio, H. Kim, A. Ruhm, J. Basu, J. Lal, S. Sinha and S. G. J. Mochrie, *Macromolecules*, 2003, **36**, 5704–5709.
10 A. R. Hillman, I. Efimov and K. S. Ryder, *J. Am. Chem. Soc.*, 2005, **127**, 16611–16620.
11 K. Dalnoki-Veress, J. A. Forrest and J. R. Dutcher, *Phys. Rev. E*, 1998, **57**, 5811–5816.
12 J. Kim and H. H. Lee, *J. Polym. Sci., Part B: Polym. Phys.*, 2001, **39**, 1122–1128.
13 P. J. Yoo, K. Y. Suh, S. Y. Park and H. H. Lee, *Adv. Mater.*, 2002, **14**, 1383–1387.
14 P. J. Yoo and H. H. Lee, *Phys. Rev. Lett.*, 2003, **91**, 154502.
15 P. J. Yoo, K. Y. Suh, H. Kang and H. H. Lee, *Phys. Rev. Lett.*, 2004, **93**, 034301(034301-034304).
16 T. Okayasu, H.-L. Zhang, D. G. Bucknall and G. A. D. Briggs, *Adv. Funct. Mater.*, 2004, **14**, 1081–1088.
17 P. J. Yoo and H. H. Lee, *Macromolecules*, 2005, **38**, 2820–2831.
18 R. Huang, *J. Mech. Phys. Solids*, 2005, **53**, 63–89.
19 S. H. Im and R. Huang, *J. Appl. Mech.*, 2005, **72**, 955–961.
20 Z. Y. Huang, W. Hong and Z. Suo, *J. Mech. Phys. Solids*, 2005, **53**, 2101–2118.
21 R. Huang and S. H. Im, *Phys. Rev. E*, 2006, **74**, 026214.
22 S. J. Kwon and J.-G. Park, *J. Phys. Chem. C*, 2007, **111**, 4404–4411.
23 H. Vandeparre, J. Leopoldes, C. Poulard, S. Desprez, G. Derue, C. Gay and P. Damman, *Phys. Rev. Lett.*, 2007, **99**, 188302(188301–188304).
24 J. C. Stover, *Optical Scattering: Measure and Analysis*, SPIE Optical Engineering Press, Bellingham, Washington, 2nd edn, 1995.
25 W. E. Wallace, J. H. van Zanten and W. L. Wu, *Phys. Rev. E*, 1995, **52**, R3329–R3332.
26 S. A. Hutcheson and G. B. McKenna, *Phys. Rev. Lett.*, 2005, **94**, 076103.
27 C. Faella, F. M. Mazzolani, V. Piluso and G. Rizzano, *J. Struct. Eng.*, 2000, **126**, 353–360.